Extension of the Eddy Dissipation Concept for turbulence/chemistry interactions to MILD combustion

Alessandro Parente[a,b,*], Mohammad Rafi Malik[a,b], Francesco Contino[c,b], Alberto Cuoci[d], Bassam B. Dally[e]

[a] *Université Libre de Bruxelles, Ecole Polytechnique de Bruxelles, Aero-Thermo-Mechanics Laboratory, Bruxelles, Belgium*
[b] *Université Libre de Bruxelles and Vrije Universiteit Brussel, Combustion and Robust Optimization Group (BURN), Bruxelles, Belgium*
[c] *Vrije Universiteit Brussel, Brussels, Department of Mechanical Engineering, Bruxelles, Belgium*
[d] *Politecnico di Milano, Department of Chemistry, Materials, and Chemical Engineering "G. Natta", Milan, Italy*
[e] *The University of Adelaide, School of Mechanical Engineering, South Australia, Australia*

Abstract

Over the past 30 years, the Eddy Dissipation Concept (EDC) has been widely applied in the industry for the numerical simulations of turbulent combustion problems. The success of the EDC is mainly due to its ability to incorporate detailed chemical mechanisms at an affordable computational cost compared to some other models. Detailed kinetic schemes are necessary in order to capture turbulent flames where there is strong coupling between the turbulence and chemical kinetics. Such flames are found in Moderate and Intense Low-oxygen Dilution (MILD) combustion, where chemical time scales are increased compared with conventional combustion, mainly because of slower reactions (due to the dilution of reactants). Recent modelling studies have highlighted limitations of the standard EDC model when applied to the simulation of MILD systems, noticeably a significant overestimation of temperature levels. Modifications of the model coefficients were proposed to account for the specific features of MILD combustion, i.e. an extension of the reaction region and the reduction of maximum temperatures. The purpose of the present paper is to provide functional expressions showing the dependency of the EDC coefficients on dimensionless flow parameters such as the Reynolds and Damköhler numbers, taking into account the specific features of the MILD combustion regime, where the presence of hot diluent and its influence on the flow and mixing fields impacts on the reaction rate and thermal field. The approach is validated using detailed experimental data from flames stabilized on the Adelaide Jet in Hot Co-flow (JHC) burner at different co-flow compositions (3%, 6% and 9% O_2 mass fraction) and fuel-jet Reynolds numbers (5,000, 10,000 and 20,000). Results show promising improvement with respect to the standard EDC formulation, especially at diluted conditions and medium to low Reynolds numbers.

Keywords: Eddy Dissipation Concept; Energy cascade model; Flameless combustion; MILD combustion; Turbulence/chemistry interactions.

*Corresponding author. Phone + 32 2 650 26 80 Fax +32 2 650 27 10 Address: Avenue F. D. Roosevelt 50, 1050 Bruxelles, Belgium.
Email address: Alessandro.Parente@ulb.ac.be (Alessandro Parente)

1. Introduction

New breakthroughs in clean energy are needed to provide our society with the necessary resources in a way that also protects the environment and addresses the climate change issue. The need for innovation is particularly important in combustion, considering that the energy derived from burning fossil fuels (coal, petroleum or natural gas) supplies over two thirds of the total world energy needs. A certain number of new combustion technologies have been proposed in recent years. Among them, Moderate or Intense Low-oxygen Dilution (MILD) [1–3] combustion is certainly one of the most promising, as it is able to provide high combustion efficiency with low pollutant emissions. This mode of combustion is achieved through the strong exhaust gas and heat recirculation, achieved by means of the internal aerodynamics of the combustion chamber in conjunction with high-velocity burners [1]. Heat recovery by preheating the oxidant stream can also help in improving thermal efficiency and maintaining the MILD regime. The resulting combustion regime features reduced local oxygen levels, distribution of reaction over the whole combustion chamber, no visible or audible flame and thus the name flameless. The temperature field is more uniform due to absence of temperature peaks, which drastically reduces NOx formation [1, 2, 4–6], while ensuring complete combustion and low CO emissions [7–10]. MILD combustion can accommodate large fuel flexibility, representing an ideal technology for low-calorific value fuels [11–14], high-calorific industrial wastes [15] as well as for hydrogen-based fuels [16, 17].

In recent years, attention has been paid to MILD combustion modelling, due to the very strong turbulence/chemistry interactions of such a combustion regime. The Damköhler number in MILD conditions usually approaches unity [17] and both mixing and chemistry need to be taken into account with appropriate turbulent combustion models. This has also been proven by Parente et al. [18], who analysed the correlation structure of MILD combustion data [19] using Principal Component Analysis (PCA) and showed that the standard flamelet approach is not suited for such combustion regime. Recently, successful predictions of different MILD combustion cases have been reported [17, 20–22] using Reynolds-Averaged Navier-Stokes (RANS) modelling and the Eddy Dissipation Concept (EDC) [23]. However, several studies of the Jet in Hot Co-flow (JHC) configuration [19] also reported that the standard EDC tends to over-predict maximum temperatures when applied to the MILD combustion regime [24, 25]. Recently, De et al. [26] carried out a detailed study on the performance of the EDC model on the Delft Jet in Hot Co-flow burner (DJHC) emulating MILD conditions. The authors showed that the model described correctly the mean velocity profiles and the Reynolds shear stress distributions, but showed significant discrepancies between measured and predicted temperatures. The mean temperature field showed systematic deviations from experimental data, due to the under-prediction of the lift-off height and the over-estimation of the maximum temperature level. This is mainly due to the over-estimations of the mean reaction rate in the EDC model. The authors showed that the prediction could be improved by adapting the standard coefficients of the classic EDC model, in particular increasing the time scale value, C_τ, from 0.4083 to 3. The results were further confirmed for the analysis of the Adelaide JHC flames with methane/hydrogen mixtures [27] and with several ethylene-based

blends [28]. Recently, Evans et al. [29] showed that adjusting the EDC coefficients C_τ and C_γ from their default value, 0.4082 and 2.1377, to 3.0 and 1.0, respectively, results in significantly improved performance of the EDC model under MILD conditions. Although the modification of the coefficients was shown to provide improved agreement between experiments and numerical simulations, it is still necessary to identify clear guidelines for the modification of the model coefficients in the context of MILD combustion, based on the specific turbulence and chemical features of such a regime. Shiehnejadhesar et al. [30] showed, for instance, that the standard EDC is not applicable for turbulent Reynolds values below 64 and proposed a hybrid Eddy Dissipation Concept/Finite-rate model calculating an effective reaction rate weighting a laminar finite-rate and a turbulent reaction rate, depending on the local turbulent Reynolds number of the flow.

The purpose of the present paper is to provide functional expressions showing the dependency of the EDC coefficients on dimensionless flow parameters such as the Reynolds and the Damköhler numbers. After a brief description of EDC and of the energy cascade model it relies on, the novel approach for the determination of the EDC coefficients will be presented. Results for the Adelaide JHC at different co-flow composition (3%, 6% et 9% O_2 mass fraction) and fuel-jet Reynolds numbers (5000, 10000 and 20000) will be presented, to assess the soundness of the current approach.

2. Eddy Dissipation Concept

The Eddy Dissipation Concept (EDC) by Magnussen [23] for turbulent combustion has found wide application for the simulation of turbulent reacting flows, especially for cases where combustion kinetics plays a major role, as it happens for MILD conditions. EDC has the advantage of incorporating detailed kinetics at a computational cost which is affordable when compared to more sophisticated models such as the transported PDF methods. This advantage is maximised when EDC is used in conjunction with *in-situ* adaptive tabulation (ISAT) [31].

According to the EDC model, combustion occurs in the regions of the flow where the dissipation of turbulence kinetic energy takes place. Such regions are denoted as fine structures and they can be described as perfectly stirred reactors (PSR). The mass fraction of the fine structures, γ_λ, and the mean residence time of the fluid within them, τ^*, are provided by an energy cascade model [32], which describes the energy dissipation process as a function of the characteristic scales:

$$\gamma_\lambda = \left(\frac{3C_{D2}}{4C_{D1}^2}\right)^{\frac{1}{4}} \left(\frac{\nu\epsilon}{k^2}\right)^{\frac{1}{4}} = C_\gamma \left(\frac{\nu\epsilon}{k^2}\right)^{\frac{1}{4}} \tag{1}$$

and

$$\tau^* = \left(\frac{C_{D2}}{3}\right)^{\frac{1}{2}} \left(\frac{\nu}{\epsilon}\right)^{\frac{1}{2}} = C_\tau \left(\frac{\nu}{\epsilon}\right)^{\frac{1}{2}} \tag{2}$$

where ν is the kinematic viscosity and ϵ is the dissipation rate of turbulent kinetic energy, k. C_{D1} and C_{D2} are model constants set equal to 0.135 and 0.5, respectively, leading to fine structure volume and residence

time constants equal to $C_\gamma = 2.1377$ and $C_\tau = 0.4083$. Fine structures are assumed to be isobaric, adiabatic perfectly stirred reactors. The mean (mass-based) source term in the conservation equation for the i^{th} species is modelled as suggested by Gran and Magnussen [33]:

$$\overline{\dot{\omega}}_i = -\frac{\overline{\rho}\gamma_\lambda^2}{\tau^* \left(1-\gamma_\lambda^3\right)} \left(\widetilde{y}_i - y_i^*\right), \tag{3}$$

where $\overline{\rho}$ denotes the mean density of the mixture, y_i^* is the mass fraction of the i^{th} species in the fine structures and $\widetilde{y}_i$ represents the mean mass fraction of the i^{th} species between the fine structures and the surrounding state (indicated as y_i^0):

$$\widetilde{y}_i = \gamma_\lambda^3 y_i^* + \left(1-\gamma_\lambda^3\right) y_i^0. \tag{4}$$

As indicated above, the expressions for γ_λ and τ^* used in the mean reaction rate for the i^{th} species are obtained from an energy cascade model, based on Kolmogorov's theory. In the following the model is briefly summarized, to highlight the main hypothesis behind it. Then, the proposed modification of the EDC standard coefficients will be presented and discussed.

2.1. Energy cascade model

The energy cascade model for EDC [32] starts with the transfer rate of mechanical energy, $w^{'}$, from the mean flow to the large turbulent eddies. The sum of the heat generated at each level, $\sum_i q_i$, is assumed to be equal to the turbulent dissipation rate ϵ. The first cascade level is characterized by a velocity scale $u^{'} = \sqrt{2/3k}$ and a length scale $L^{'}$, giving a strain rate $\omega^{'} = u^{'}/L^{'}$, and it represents the whole turbulence spectrum because it contains the effect of smaller scales. In the energy cascade model, it is assumed that the strain doubles at each level, so that $\omega^{''} = u^{''}/L^{''} = 2\omega^{'}$. The strain rate at level n is $\omega_n = 2\omega_{(n-1)}$. In the original model formulation, the last level is described by scales ω^*, u^*, L^*, which are considered to be of the same order of Kolmogorov scales, ω_k, u_k, L_k.

The rate of production of mechanical energy, w_i, and the rate of viscous dissipation, q_i, at each level of the cascade are expressed [32] in analogy to the production and dissipation terms appearing in the equation of turbulent kinetic energy, k. This implies, for level n:

$$w_n = \frac{3}{2} C_{D1} \omega_n u_n^2 = \frac{3}{2} C_{D1} \frac{u_n^3}{L_n}, \tag{5}$$

$$q_n = C_{D2} \nu \omega_n^2 = C_{D2} \nu \frac{u_n^2}{L_n^2} \tag{6}$$

and, by the conservation of energy

$$w_n = q_n + w_{n+1}. \tag{7}$$

At the fine structure level, where reaction occurs, the energy is dissipated into heat,

$$w^* = \frac{3}{2} C_{D1} \frac{u^{*3}}{L^*} = q^* = C_{D2} \nu \frac{u^{*2}}{L^{*2}}. \tag{8}$$

In the original energy cascade formulation, the value of C_{D2} was selected as best fit for several types of flow, whereas C_{D1} was chosen using the approximation that for $Re >> 1$ nearly no dissipation takes place at the highest cascade level. This implies:

$$\varepsilon = w^{'} = q^{'} + w^{''} = w^{''} = \frac{3}{2} C_{D1} \frac{u^{'3}}{L^{'}}. \tag{9}$$

Under this assumption, a relation can be found between C_{D1} and the $k-\epsilon$ turbulent model constant C_{μ}, *via* the definition of the turbulent viscosity, ν_T:

$$u^{'} L^{'} = \frac{3}{2} C_{D1} \frac{u^{'4}}{\epsilon} = \frac{2}{3} C_{D1} \frac{k^{'2}}{\epsilon}. \tag{10}$$

Considering the definition of ν_T in the $k-\epsilon$ turbulent model, $\nu_T = c_{\mu} \frac{k^{'2}}{\epsilon}$, we conclude that $2/3 C_{D1}$ corresponds to the constant $C_{\mu} = 0.09$, which gives $C_{D1} = 0.135$. On the other hand, summing up all level contributions to dissipation, and performing an energy balance on the last energy level, two additional relations are found [32]:

$$\epsilon = \frac{4}{3} C_{D2} \nu \frac{u^{*2}}{L^{*2}} \tag{11}$$

$$\epsilon = 2 C_{D1} \frac{u^{*3}}{L^{*}}. \tag{12}$$

Combining Equations (11) and (12), we conclude that the fine structure scale is of the same order of the Kolmogorov one:

$$Re^{*} = \frac{u^{*} L^{*}}{\nu} = \frac{2}{3} \frac{C_{D2}}{C_{D1}} = 2.5. \tag{13}$$

The classical cascade model described here has been developed for high Reynolds number flows, with clear separation between turbulent scales. However, in MILD combustion, there is no longer a clear separation between large and small scales of turbulence, and reaction can occur over a wide range of scales [34]. Therefore, the chemical reactions proceed in a thick distributed reaction zone comparable to the integral length scale, leading to a modification of the characteristic scales of the reaction structures, due to the transfer of energy to higher frequencies than those of the reacting structures in the spectrum. It is therefore necessary to revise the cascade model, to deal with the specific features of the MILD combustion regime, and clarify the dependency of the energy cascade parameters on the flow and reaction structure characteristics, using the Reynolds and Damköhler numbers.

2.2. Determination of energy cascade coefficients in MILD combustion

In MILD combustion, the dilution and preheating of the reactants generate a unique "distributed" reaction zone [34]. The system evolves towards perfectly mixed conditions and the reaction process is characterized by a Damköhler number approaching unity. As pointed out in the introduction, this has led several research groups to modify the classic EDC model coefficients to achieve better predictions of experimental data. In

particular, the choice of the coefficients proposed by Evans et al. [29] has interesting implications for what concerns the fine structure characteristics. Using the values of 3.0 and 1.0 for C_τ and C_γ, respectively, in Equation (13), a characteristic Reynolds number $Re^* = 4$ is obtained, which indicates that the reacting structures in MILD combustion have larger characteristic dimensions than in traditional combustion systems. This was recently confirmed by the analysis of Minamoto et al. [34], who pointed out that reacting regions in MILD combustion are distributed over a good portion of the computational domain and the interaction between reaction zones leads to an appearance of distributed reaction, resulting in relatively uniform temperature distribution.

We assume that the MILD combustion happens in the so-called Distributed Reaction Regime, to base our revision of the standard cascade model. Such a combustion regime is associated mainly with small-scale, high-intensity turbulence. In such a regime, $u' >> S_L$ and $L^{'} < \delta_L$, meaning that Kolmogorov scales are able to enter and to thicken the preheating zone and, possibly, the reaction region, leading to a thickened and distributed flame structure [35, 36]. In such a scenario, it is appropriate to estimate the characteristic speed of the reacting fine structures from the turbulent flame speed. The validity of such hypothesis requires that a flame front can be still defined at the characteristic scales of the reacting structures, and this is indeed the case for the regime under investigation, given its distributed nature determined by the high-intensity turbulence. When dealing with this regime, it is a common practice to: i) model the effects of turbulence on combustion as enhancement of heat and mass transport; ii) employ the classic expression by Damköhler for turbulent flame speed, S_T [36, 37]:

$$S_T = S_L \sqrt{\frac{\alpha_T + \alpha}{\alpha}} \approx S_L \sqrt{\frac{\nu_T + \nu}{\nu}} = S_L \sqrt{Re_T + 1} \tag{14}$$

where $Re_T = k^2/(\nu\epsilon)$ is the turbulent Reynolds number. The use of premixed quantities such as the laminar flame speed is justified by the large degree of partial premixing occurring in MILD conditions. The very strong recirculation determines a modification of the reaction region which evolves to perfectly stirred reactor (PSR) conditions. The nature of reacting structures and the suitability of existing modelling paradigms in MILD combustion has been recently investigated by Minamoto and Swaminathan [38]. They showed that MILD reaction zones are highly-convoluted, contorted and pancake-like structures, spread over a large portion of the computational domain resulting in a relatively broad reaction zone. By means of a systematic comparison between numerical simulations and DNS data, the authors showed that the PSR modelling paradigm is applicable in the (RANS and LES) modelling of MILD combustion, as also demonstrated in [39, 40]. Based on this observation, the use of Equation (14) appears a good first-order estimate of the reacting structure characteristic velocity for MILD conditions, and it can be used to infer the dependency of the energy cascade model coefficients C_{D1} and C_{D2} on the dimensionless reacting flow numbers.

From Eq. (11), we know that $\epsilon \propto C_{D2}\nu u^{*2}/L^{*2}$. Considering that u^* is the characteristic speed of the turbulent reacting fine structures, i.e. $u^* \sim S_T = S_L\sqrt{Re_T + 1}$, one gets from Eq. (14):

$$\epsilon \propto C_{D2}\nu\frac{u^{*2}}{L^{*2}} = C_{D2}\nu\frac{S_L^2\left(Re_T+1\right)}{L^{*2}}. \tag{15}$$

The length scale L^* can be interpreted as the characteristic linear dimension of the reacting fine structures, being the reactions distributed over many turbulent length scales. This implies that the ratio L^*/S_L indicates a characteristic chemical time scale, τ_c, of the reacting structures, in line with the classic treatment of turbulent premixed flames [36]. Consequently, τ_c can be expressed as a function of the Kolmogorov mixing time scale, τ_η, using the flow Damköhler number. Thus, dissipation can be expressed as:

$$\epsilon \propto \frac{\left[C_{D2}\nu\left(Re_T+1\right)\right]}{\tau_c^2} = \frac{\left[C_{D2}\nu\left(Re_T+1\right)Da_\eta^2\right]}{\tau_\eta^2}. \tag{16}$$

Here, the pertinent mixing time scale for comparison is the Kolmogorov one, as indicated in the original energy cascade model by Ertesvåg and Magnussen [32], explaining the use of the symbol Da_η, to indicate that the Damköhler number is evaluated at the Kolmogorov scale η_k, $Da_\eta = \tau_\eta/\tau_c$. Such a choice is motivated by the need of comparing the reaction process occurring in the fine structures to the molecular mixing process at the Kolmogorov scale. The problem could be also treated by introducing the Karlovitz (Ka) number, which intrinsically adopts the Kolmogorov scale, leading to an equivalent formulation. However, the interpretation in terms of Damköhler number appears more immediate, being the observed Da_η number for MILD systems of order unity [41]. Expressing $\tau_\eta = (\nu/\epsilon)^{\frac{1}{2}}$, we get the following dependency of C_{D2} on Re_T and Da_η:

$$C_{D2} \propto \frac{1}{\left[Da_\eta^2\left(Re_T+1\right)\right]}. \tag{17}$$

Given the definition of C_τ (Eq. (2)), we obtain:

$$C_\tau \propto \frac{1}{Da_\eta\sqrt{Re_T+1}} \tag{18}$$

Equation (18) provides a theoretical basis and confirms the recent findings in [26, 27]. In particular, it shows that for combustion regimes characterized by low Damköhler numbers, the fine structure time coefficient should be increased, to account for: i) the wider reaction regions; ii) the reduction of driving forces due to the smoothed gradients; and iii) the reduction of temperature due to higher dilution. Moreover, Eq. (18) also introduces an explicit dependence on the turbulent Reynolds number, indicating that for decreasing Re_T the aforementioned phenomena become even more relevant.

A similar procedure can be carried out to determine the dependency of C_γ on Re_T and Da_η. From Eq. (13) we can find a relationship between C_{D2} and C_{D1}, $C_{D2}/C_{D1} = 3/2Re^* = \frac{3}{2}\frac{u^*L}{\nu}$. Using Eq. (14) for u^*, we get

$$\frac{C_{D2}}{C_{D1}} = \frac{3}{2}S_L\sqrt{\frac{\nu_T+1}{\nu^2}}L^*, \tag{19}$$

and, since $S_L \propto \sqrt{\nu/\tau_c}$ [36], the ratio C_{D2}/C_{D1} can be expressed as

$$\frac{C_{D2}}{C_{D1}} = \frac{3}{2}\frac{L^*}{S_L}\frac{\sqrt{\frac{\nu_T}{\nu}+1}}{\tau_c} \propto \sqrt{Re_T+1}. \tag{20}$$

Based on the definition of C_γ(Eq. 1), the following expression is found:

$$C_\gamma = \left(\frac{3C_{D2}}{4C_{D1}^2}\right)^{\frac{1}{4}} \propto \left[\frac{(Re_T+1)}{C_{D2}}\right]^{\frac{1}{4}} \propto Da_\eta^{\frac{1}{2}} \left(Re_T+1\right)^{\frac{1}{2}} \tag{21}$$

which indicates that the fine structure coefficient should be decreased for decreasing Re_T and Da_η. This result can be interpreted considering that for low Re_T and Da_η the fine structures are more distributed and their local mass fraction decreases. Moreover, it is important to note that the dependency on the Damköhler number for such a coefficient is less important than for C_τ.

3. Validation test cases

In order to validate the proposed approach, data are needed at different Re_T and Da_η. To this end, the Adelaide Jet in Hot Co-flow burner [19] represents an ideal test-case for our purposes, thanks to the availability of detailed experimental measurements (temperature and species compositions) at different oxygen levels in the co-flow, ranging from 3% to 9%, allowing to control the system Da_η number, and at different fuel jet Reynolds numbers (5000, 10000 and 20000). The MILD combustion burner (Figure 1) consists of a central insulated fuel jet (Ø4.6mm) within an annular co-flow (Ø82mm) of hot exhaust products from a secondary burner mounted upstream of the jet exit plane. The O_2 level in the co-flow is controlled by the constant flow-rate secondary porous burner. The ratio of the co-flow air/nitrogen was varied to give coflow O_2 levels of 3% (HM1), 6% (HM2) and 9% (HM3) (mass fractions), while the temperature and exit velocity were kept constant at 1300 K and 3.2 m/s. The jet Reynolds number was varied for the 3% O_2 level, from 5000 (HM1-5k) to 10000 (HM1) and 20000 (HM1-20k). The available data consist of mean and root mean square (rms) of temperature and mass fractions of major (CH_4, H_2, H_2O, CO_2, N_2 and O_2) and minor species (NO, CO and OH).

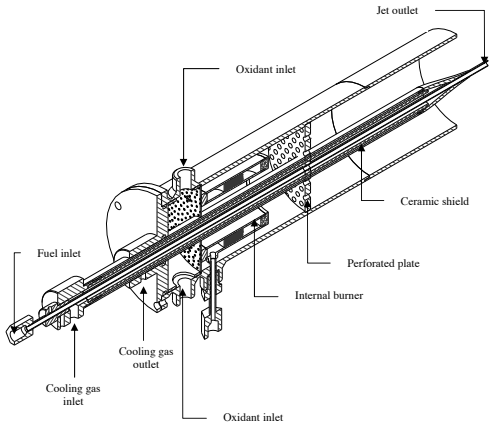

Figure 1: Schematic of the Jet in Hot Co-flow burner [19].

Numerical simulation were carried out using the Ansys FLUENT 14.5 CFD commercial code. A two-dimensional steady-state simulation of the physical domain was considered due to the symmetry of the system.

The computational domain is 1000 mm in the axial direction and 120 mm in the radial direction from the jet exit. The mesh is structured and non-uniform with about 20,000 cells, to provide high resolution in the reaction zone and save computational effort elsewhere. Two additional meshes were considered to evaluate the Grid Convergence Index (GCI), which gives a measure of deviation from the asymptotic numerical value [42]. A GCI value of about 2% was obtained for temperature and major species, using the base grid and the KEE-58 mechanism [43].

Velocity-inlet boundary conditions are specified at the inlets, whereas pressure-outlet conditions are applied at the boundaries assuming ambient air back-flow conditions, being the flame non-confined. Turbulence is modelled using a modified $k-\epsilon$ model, with the $C_{\epsilon 1}$ parameter modified to a value of 1.60 for self-similar round jets [44]. Particular attention was given to the specification of the turbulence level of the co-flow, as previous studies [25, 27] indicated the very strong effect of turbulence intensity on the mixing level and the quality of the predictions.

The KEE-58 mechanism is considered in the present study in combination with EDC model in its standard formulation and using the modifications proposed in Section 2.2. The choice of the KEE-58 mechanism was motivated by the relatively low computational cost associated with this mechanism compared to more complete ones such as the GRI-2.11 and GRI-3.0 mechanisms [45, 46]. Figure 2 shows a comparison between the measured and calculated temperature profiles, providing a benchmark of the three mechanisms. Results show negligible differences between the KEE-58 and GRI-2.11/GRI-3.0 mechanisms, below 2-3% in all cases, thus justifying the use of the less computational expensive KEE-58 scheme for the present investigation.

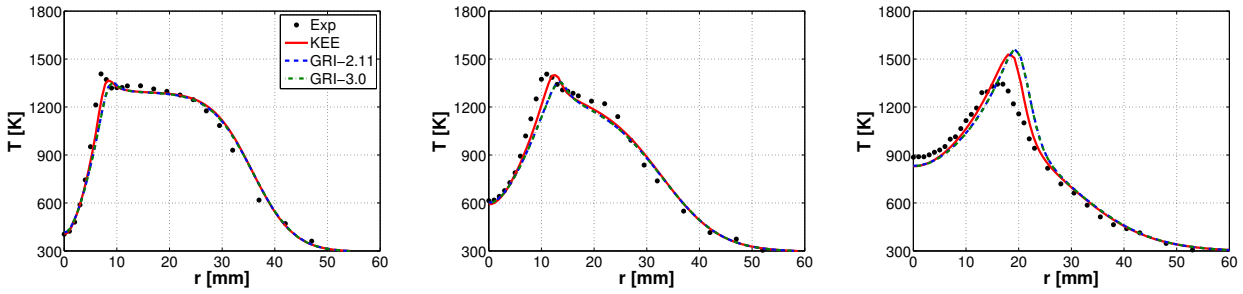

(a) HM1, z =30mm (b) HM1, z =60mm (c) HM1, z =120mm

Figure 2: Comparison between measured and computed mean temperature for flame HM1 at three axial locations using the standard EDC with three chemical kinetic mechanisms, KEE-58 (red), GRI-2.11 (blue) and GRI-3.0 (green).

Differential diffusion is taken into account by calculating binary diffusion coefficients from the kinetic theory, and the discrete ordinate (DO) method together with the Weighted-Sum-of-Gray-Gases (WSGG) model is used for radiation. Second-order upwind schemes are employed for all equations and the SIMPLE algorithm is used for pressure-velocity coupling.

3.1. Determination of EDC coefficients

The proposed approach for the determination of EDC parameters is tested in two different ways, using global or local coefficients.

In the first approach, global coefficients are determined using Equations (18) and (21). The determination of the modified model coefficients requires the knowledge of characteristic Re_T and Da_η numbers for the system of interest. Re_T can be directly computed, based on the estimated values of the turbulent kinetic energy, k, and dissipation rate, ϵ, of the fuel jet, $Re_T = k^2/(\nu\epsilon)$. On the other hand, the estimation of Da_η requires, in principle, the *a priori* knowledge of the solution. Isaac et al. [41] recently developed an approach for the calculation of chemical time-scales of turbulent combustion data with detailed chemistry, based on the down-sizing of the chemical source term Jacobian using Principal Component Analysis. The analysis was demonstrated on the HM1, HM2 and HM3 flames, for which values of Da_η of 0.775, 1.15 and 1.4 [41] were estimated, respectively. Therefore, the availability of characteristic Re_T and Da_η numbers allow us to find the values of C_τ and C_γ, as indicated in Table 1. For the constant Reynolds number (10,000), oxygen varying flames (HM1, HM2 and HM3), the variation of the coefficients C_τ and C_γ is only due to the variation of Da_η . On the other hand, for the Reynolds varying HM1 flames at $y_{O_2} = 0.03$ (HM1-5k, HM1 and HM1-20k), both Re_T and Da_η change (due to the change in turbulent dissipation rate, being $\tau_\eta = (\nu/\epsilon)^{\frac{1}{2}}$), as indicated in Table 1. It can be observed that the approach requires the determination of a reference case, for which standard values of EDC coefficients are applied. For C_τ, the reference was set through extrapolation of the Da_η values from diluted ($y_{O_2} = 0.03$) to standard air ($y_{O_2} = 0.232$) conditions, using the estimated Da_η values for HM1-HM3 flames. This gave a reference Da_η of 2.8, at which $C_\tau = 0.4083$. In the present investigation, the focus is initially put on the variation of the coefficient C_τ. This allows to better assess the soundness of the proposed approach, since the observed trends can be more easily explained and linked to a single parameter variation. The effect of the simultaneous variation of C_τ and C_γ is also investigated.

Table 1: C_τ and C_γ as a function of global Re_T and Da_η values.

Flame	$\boldsymbol{Re_T}$	$\boldsymbol{Da_\eta}$	$\boldsymbol{C_\tau}$	$\boldsymbol{C_\gamma}$	Flame	$\boldsymbol{Re_T}$	$\boldsymbol{Da_\eta}$	$\boldsymbol{C_\tau}$	$\boldsymbol{C_\gamma}$
HM1	400	0.78	1.47	1.90	HM1-5k	225	1.20	1.25	1.78
HM2	400	1.15	1.00	2.14	HM1	400	0.78	1.47	1.90
HM3	400	1.4	0.82	2.14	HM1-20k	760	0.50	1.77	2.00

When using local coefficients, the values of Re_T and Da_η must be computed locally for each cell. The procedure is straightforward for the turbulent Reynolds number, which can be easily computed using the local value of turbulent kinetic energy and turbulent dissipation rate.. As far as the Damköhler number is concerned, its evaluation requires the estimation of the leading chemical time scale, τ_c, through the analysis and decomposition of the Jacobian of the system chemical source terms [41]. Such a procedure can be very expensive for the on-the-fly determination of the EDC parameters. Therefore, the estimation of the controlling

chemical time scale was based on a one-step chemistry [47], obtaining temperature and the necessary species concentrations from the detailed chemical mechanism. This approach was found to provide reasonable good predictions for the system under investigation in [41], being the one-step chemistry applied on accurate thermal and concentration fields. Once τ_c, is available, Da_η is simply computed from the definition $Da_\eta = \tau_\eta/\tau_c$, where $\tau_\eta = (\nu/\epsilon)^{\frac{1}{2}}$. The use of local coefficients required the modification of original EDC model. Indeed, Ansys FLUENT does not allow the change of the coefficients locally. Therefore, two User-Defined Functions (UDF) were used: one for the calculation of the EDC coefficients based on local values of the Reynolds and Damköhler numbers; and the second to compute the net formation rate for each species based on the EDC formulation. A contour plot showing the Re_T and Da_η numbers for the system under investigation is shown in Figure 3. The typical distribution of C_τ and C_γ for the flame under investigation

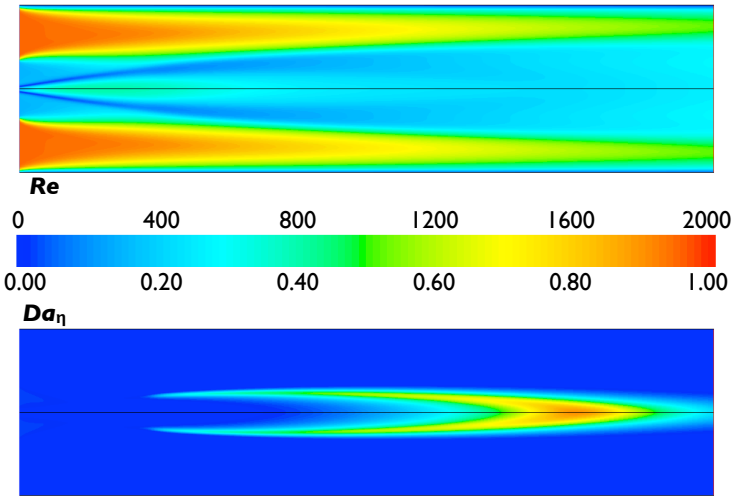

Figure 3: Characteristic Re_T and Da_η distribution for the JHC system. The horizontal axis denotes the axial direction. O_2 level in the co-flow: 3%. Fuel-jet Reynolds number:10,000.

is shown in Figure 4. The same formulation of the local coefficients was employed for all calculations, to avoid any fitting/optimization of the results for specific operating conditions. Figure 4a-b shows that the EDC local coefficients are limited to their standard values, i.e. $C_\gamma = 2.1377$ and $C_\tau = 0.4083$. Figure 4c shows the Re^* from the modified local coefficients, indicating value in the range 3-5 in the ignition region, in agreement with the modified EDC model recently proposed by Evans et al. [29]. The distribution of C_γ (Figure 4b) is due to the fact that for very low values of Da_η, the C_γ was set to its standard value, to ensure proper ignition. The threshold value for Da_η was set to 0.01 in the present work; however, it was verified that the results were insensitive to a variation of 50% around this value, to ensure the robustness of such a choice. The need of a threshold value is mostly related to the approach used for the calculation of Da_η, based on a one-step chemistry. This is very practical for the on-the-fly calculation of the model coefficients, but it results in unrealistic estimations of Da_η values outside of the flame region.

4. Results

This section describes the results obtained for the test cases at varying co-flow concentrations and fuel-jet Reynolds numbers, with the objective of assessing the effect of the proposed modification of the EDC coefficients on the results. First, the results of the approach based on global coefficients will be presented and discussed. Then, the results of the local coefficients approach will be shown. To better assess the quantitative agreement between model predictions and measurements, the results shown in the present section do not only indicate the mean observed value of the scalar under consideration (temperature and species mass fractions) but also the 95% confidence for the true mean value, μ, associated to the measurements, $\overline{y}_e$, calculated as [48]:

$$\overline{y}_e - t_{\frac{\alpha}{2},\nu}\frac{s}{\sqrt{n}} < \mu < \overline{y}_e + t_{\frac{\alpha}{2},\nu}\frac{s}{\sqrt{n}} \tag{22}$$

where $t_{\frac{\alpha}{2,},\nu}$ is the $\left(1-\frac{\alpha}{2}\right)$ quantile of Student's t-distribution defined by the n experimental observations. with $\nu = n-1$ degrees of freedom, and s is the sample standard deviation,

$$s = \left[\frac{1}{n-1}\sum_{i=1}^{n}\left(y_e^i - \overline{y}_e\right)^2\right]^{\frac{1}{2}}. \tag{23}$$

The calculation of the confidence intervals was made possible by the availability of a large number of observations y_e^i (~ 500) for each measurement point.

4.1. Modified EDC - global coefficients

Figure 5 shows the radial temperature profiles at different axial locations, for flames HM1 (a-c), HM2 (d-f) and HM3 (g-i). The modified EDC results shown are obtained through modification of the coefficient C_τ. It can be observed that the adjustment of C_τ determines a generalized improvement of predictions: the temperature over-prediction is strongly reduced and the radial temperature distribution is better captured. At high axial distances, i.e. $z = 120$ mm, the behaviour of the model remains unsatisfactory, although an improvement is noticeable with respect to the standard EDC model. To further confirm the qualitative analysis based on the observation of Figure 5, the relative error in the prediction of the maximum temperature at different axial locations is shown in Table 2. The peak temperature for the HM1 flame at $z = 120$ mm decreased from 1716 K to about 1526 K, the experimental value being 1343 K, implying a reduction of the relative error from 28% to 14%. Similar improvements are observed for HM2 and HM3 flames, for which the error decreases from to 26% to 19% and from 20% to 16%, respectively. The trend is confirmed at all axial distances and for all flames, with the exception of location z =30 mm for HM1 flame, where the performances of standard and modified models are comparable. In particular, the modified model performs remarkably well at $z = 60$ mm when compared to standard EDC settings. Interestingly, the coefficient modification appears more beneficial as the departure from conventional combustion conditions is more important. This is of straightforward interpretation, being the developed model based on theoretical considerations valid in

Table 2: Relative error on maximum temperatures at different axial locations of standard and modified EDC models for flames at varying oxygen concentration (HM1-HM3).

	HM1, Relative error on T_{max} [%]			
z [mm]	Std	Global coefficients		Local coefficients
		C_τ	C_τ & C_γ	
30	0.91	2.90	3.80	3.48
60	5.00	0.50	3.60	1.75
120	27.80	13.60	5.60	9.35
	HM2, Relative error on T_{max} [%]			
z [mm]	Std	Global coefficients		Local coefficients
30	8.20	4.00		1.84
60	10.80	6.10		4.37
120	25.90	18.50		2.27
	HM3, Relative error on T_{max} [%]			
z [mm]	Std	Global coefficients		Local coefficients
30	6.00	2.40		8.56
60	8.50	5.10		10.49
120	20.30	15.50		3.08

the framework of distributed reaction regime limit. The quantitative results shown in Table 2 support the proposed modification of the EDC coefficients and provide a theoretical basis to previous results obtained by other authors [26–28].

The availability of experimental data at different fuel-jet Reynolds numbers allows evaluating the performances of the proposed model when modifying the Reynolds number at the conditions of highest dilution ($y_{0_2} = 0.03$). The fuel-jet Reynolds number is varied from 5,000 (HM1-5k) to 20,000 (HM1-20k), resulting in different characteristic turbulent Reynolds numbers with respect to the base case (HM1) (Table 1). Figure 7 shows the radial temperature profiles at different axial locations, for flames HM1-5k (a-c) and HM1-20k (d-f). Results confirm the trend observed for the varying oxygen cases, indicating that the modified model yields improved predictions of temperature distribution at both Reynolds numbers. This is also proved by the quantitative results in Table 3, which shows in particular remarkable performances for the HM1-5k flame.

The HM1-20k flame deserves a separate discussion. The experimental data show a strong temperature reduction for increasing distance from the burner nozzle, at $z = 120$ mm, due to the partial extinction of the flame caused by the increased jet velocity. This phenomenon can be clearly observed in Figure 6, which shows the instantaneous temperature measurements as a function of the mixture fraction for the HM1 flames at Reynolds numbers 10,000 (a) and 20,000 (b), respectively. The amount of partial extinction and re-ignition is significantly higher at higher Reynolds number, as indicated by the large data scatter in Figure

6b compared to Figure 6a. This phenomenon is not captured by the standard EDC formulation, which results in a significant over-prediction of the temperature levels at $z = 60$ mm and $z = 120$ mm (Table 3). The modification of the EDC model coefficients improves the model predictions, as indicated by the error metrics in Table 3 and the radial temperature distributions in Figure 7d-f. However, with the modified EDC formulation, the flame extinguishes for axial distances higher than $z = 120$ mm and the model is unable to reproduce the re-ignition observed experimentally. This indicates that the combination of RANS modelling with the EDC approach is not adequate to model the HM1-20k flame, as the model provides either a stable flame with temperature levels significantly higher than those observed experimentally or an extinguishing but not re-ignition flame. It was attempted to model the HM1-20k flame using the transported PDF approach, but this also resulted in global extinction, as indicated in the literature [49]. This suggests that more complex approaches, i.e. unsteady simulations and/or LES, should be employed to model such a flame.

Table 3: Relative error on maximum temperatures at different axial locations of standard and modified EDC models for flames at varying fuel-jet Re numbers (HM1-5k and HM1-20k).

	HM1-5k, Relative error on T_{max} [%]	
z [mm]	C_τ=0.4083	C_τ=1.96
30	5.90	1.86
60	11.80	3.31
120	20.90	10.35
	HM1-20k, Relative error on T_{max} [%]	
z [mm]	C_τ=0.4083	C_τ=1.07
30	0.74	2.95
60	16.00	3.21
120	82.20	10.22

The effect of the simultaneous change of the two model coefficients, C_τ and C_γ, on the results was also investigated. Figure 8 shows the radial temperature profiles at $z = 30$ mm (a), $z = 60$ mm (b) and $z = 120$ mm (c) for the HM1 flames, providing a benchmark between all the tested models. It appears evident that the modification of C_γ has a minor influence at axial distances $z < 60$ mm, whereas a clear effect can be observed at z =120 mm, where the over-prediction of the temperature distribution is further reduced, leading to better agreement between measurements and simulations with respect to the case based on the modification of the coefficient C_τ. This is confirmed quantitatively by the results in the first columns of Table 2, which shows a relative error metric for maximum temperature decreasing from 13.6% to about 5%, when modifying simultaneously the two model coefficients.

To further assess the potential improvement associated with the use of modified coefficients, the standard and modified formulation are compared against the experimental observation of major (CO_2 and H_2O) and minor species (CO) and radicals (OH). Figure 9 shows the radial profile of CO mass fraction at different

axial locations for the HM1 (a-c), HM2 (d-f) and HM3 (g-i) flames, using the standard EDC formulation and the modified one with global coefficients. The observed improvement in temperature distributions is expected to yield better agreement for observed and measured CO mass fractions. At $z = 30$ mm for the HM1 case (Figure 9a), the modified model formulation provides better prediction only far from the axis, underestimating the CO level at the centerline with respect to the standard model. On the other hand, the improvements are significant and more clearly visible for the HM2 and HM3 (Figure 9d and Figure 9g respectively), particularly at the centerline. The same conclusions can be drawn for the CO profiles at $z = 60$ mm and at $z = 120$ mm. A similar analysis for the OH radical (Figure 10) shows that the use of the modified coefficients provides improved results for increasing distances from the burner exit, whereas close to the burner the OH peak is better captured by the standard EDC model. Moreover, it is possible to observe that both default and modified models perform poorly at $z = 120$ mm. We mainly attribute this behaviour to the intermittent localized flame extinction, documented in the literature for the flames under investigation [24, 27], especially at diluted conditions. While the EDC model is capable of capturing the flame lift-off, it fails in capturing such non-equilibrium phenomena.

The radial profiles of major species, i.e. CO_2 and H_2O, indicate that the use of the modified model always results in better predictions than the standard model. Figures 11 and 12 indicate that the modified model better captures the observed values close to the axis, as well as at the peak value and values far from the axis.

It is important to note that the analysis of the results cannot be only limited to the role of the modified EDC coefficients, but it should include further investigations on the influence of the turbulence model and the kinetic mechanism. The objective of the present paper is to assess, for a given configuration, if the proposed model for the modification of the EDC coefficients results in explainable and consistent trends, which appears evident from the results.

4.2. Modified EDC - local coefficients

Finally, we analyzed the effect of local coefficients on the results. The objective is to verify that the on-the-fly calculation of the EDC coefficients provides results in agreement with those obtained using the modified global coefficients, without the need for an *a priori* knowledge of the results, which would make the practical use of the theory developed in the present paper quite challenging. Figure 13 shows the radial temperature profiles at different axial locations, for flames HM1 (a-c), HM2 (d-f), HM3 (g-i) and HM1-5k (j-l), using the modified EDC formulation with globally and locally (in each grid cell) computed coefficients, respectively. One general observation that can be made from these plots is that the results obtained with a local evaluation of the coefficients compares very well with the results obtained using modified global coefficients, providing thus improved results with respect to the standard EDC formulation. In some cases, far from the burner nozzles, the results obtained using the local coefficients show even better agreement with the experimental data. The same conclusions hold also for species distributions. In particular, the OH radial profiles at $z = 120$ mm for flames HM1-HM3 (Figure 14) indicate that, while the results using global and

local coefficients are very similar for the HM1 flame, there is a substantial improvement in OH prediction when adopting local coefficients. This indicates that for the very diluted conditions (HM1), the use of the local coefficients does not solve the problem related to the inability of EDC of capturing the localized flame extinction. However, for the less diluted, more stable conditions (HM2-HM3), a local evaluation of the EDC coefficients gives improved results in the contracted region of the flame, where the use of global constants (tuned using the fuel jet characteristics) over-estimates the reaction rates.

We can therefore conclude that the use of local coefficients for EDC is a viable option for the practical implementation of the proposed functional dependencies between the EDC coefficients and the dimensionless Re_T and Da_η numbers. The use of local coefficients has clear advantages over the use of global ones, as it does not require prior knowledge of the characteristic dimensionless numbers (Re_T and Da_η) in the system. Moreover, it should be stressed out that the use of local coefficients does not have an impact on the simulation time, as the latter is dominated by the chemistry integration time. This method can thus be seen as an effective way for on-the-fly calculations.

5. Conclusions

The Eddy Dissipation Concept (EDC) for turbulent combustion is widely used to model turbulent reacting flows where chemical kinetics may play an important role, as it is the case for MILD combustion. However, recent investigations have pointed out the limitations of the approach for such a regime. The present paper proposes a modification of the EDC model coefficients to allow its application in the context of MILD conditions. The main findings of the present work can be summarized as follows:

- The energy cascade model, on which EDC is founded, was revisited in the limit of the distributed reaction regime, to derive explicit dependencies between the EDC model coefficients and the Reynolds and Damköhler dimensionless numbers.

- The proposed approach was validated on several data sets collected on the JHC burner with different co-flow composition (3%, 6% et 9% O_2 mass fraction) and fuel-jet Reynolds numbers (5,000, 10,000 and 20,000). For the 20,000 Reynolds number case, the modification of the EDC model coefficients improves the model predictions close to the burner. However, the model is unable to reproduce the re-ignition observed experimentally at higher axial distance. This does not appear related to the EDC model itself, rather to the RANS modelling limitations.

- The proposed approach was first validated using modified global coefficients, determined on the basis on available simulation results. Results based on the variation of the time scale coefficient, C_τ, show promising improvement with respect to the standard EDC formulation close to the burner, especially at diluted conditions and medium to low Reynolds numbers, for both temperature and species measurements. Moreover, the simultaneous modification of the time scale, C_τ, and the mass fraction

coefficients, C_γ, leads to improvements in the model predictions at large axial distances from the burner exit.

- The proposed approach was then validated using a local evaluation of the EDC model coefficients, using the local values of Re_T and Da_η numbers. The Re_T value was estimated from the local values of turbulent kinetic energy and dissipation rate, while Da_η was obtained from a one-step reaction, using the temperature and species concentrations coming from the detailed mechanism employed for the gas-phase reactions. Results from the local approach are comparable or superior to those provided via the modification of the global coefficients, thus indicating the viability of the approach.

Future work will investigate the influence of the turbulence model and kinetic mechanism on the predictions and their impact on the modified coefficients, using validation data from experiments and Direct Numerical Simulations. Moreover, more accurate approaches for the determination of the chemical time-scale and Da_η number will be investigated.

Acknowledgements

The first and second Authors would like to ackowledge the support of Fédération Wallonie-Bruxelles, via "Les Actions de Recherche Concertée (ARC)" call for 2014-2019, to support fundamental research.

[1] J. A. Wünning, J. G. Wünning, Progress in Energy and Combustion Science 23 (1997) 81–94.

[2] A. Cavaliere, M. de Joannon, Progress in Energy and Combustion Science 30 (2004) 329–366.

[3] A. K. Gupta, Journal of Engineering for Gas Turbines and Power 126 (2004) 9–19.

[4] G. M. Choi, M. Katsuki, Energy Conversion and Management 42 (2001) 639–652.

[5] B. B. Dally, E. Riesmeier, N. Peters, Combustion and Flame 137 (2004) 418–431.

[6] G. G. Szego, B. B. Dally, G. J. Nathan, Combustion and Flame 154 (2008) 281–295.

[7] M. de Joannon, P. Sabia, G. Sorrentino, A. Cavaliere, Proceedings of the Combustion Institute 32 (2009) 3147 – 3154.

[8] M. de Joannon, G. Sorrentino, A. Cavaliere, Combustion and Flame 159 (2012) 1832 – 1839.

[9] A. Mardani, S. Tabejamaat, S. Hassanpour, Combustion and Flame 160 (2013) 1636 – 1649.

[10] C. Zou, S. Cao, Y. Song, Y. He, F. Guo, C. Zheng, Fuel 130 (2014) 10 – 18.

[11] S. E. Hosseini, M. A. Wahid, Energy Conversion and Management 74 (2013) 426 – 432.

[12] A. Abuelnuor, M. Wahid, S. E. Hosseini, A. Saat, K. M. Saqr, H. H. Sait, M. Osman, Renewable and Sustainable Energy Reviews 33 (2014) 363 – 370.

[13] G. Mosca, D. Lupant, A. Gambale, P. Lybaert, in: Proceedings European Combustion Meeting, Lund, Sweden.

[14] S. E. Hosseini, G. Bagheri, M. A. Wahid, Energy Conversion and Management 81 (2014) 41 – 50.

[15] M. Derudi, A. Villani, R. Rota, Industrial & Engineering Chemistry Research 46 (2007) 6806–6811.

[16] P. Sabia, M. de Joannon, S. Fierro, A. Tregrossi, A. Cavaliere, Experimental Thermal and Fluid Science 31 (2007) 469–475.

[17] A. Parente, C. Galletti, L. Tognotti, International Journal of Hydrogen Energy 33 (2008) 7553 – 7564.

[18] A. Parente, J. Sutherland, B. Dally, L. Tognotti, P. Smith, Proceedings of the Combustion Institute 33 (2011) 3333 – 3341.

[19] B. B. Dally, A. N. Karpetis, R. S. Barlow, Proceedings of the Combustion Institute 29 (2002) 1147–1154.

[20] C. Galletti, A. Parente, M. Derudi, R. Rota, L. Tognotti, International Journal of Hydrogen Energy 34 (2009) 8339 – 8351.

[21] A. Parente, C. Galletti, L. Tognotti, Proceedings of the Combustion Institute 33 (2011) 3343–3350.

[22] A. Parente, Galletti, J. Riccardi, M. Schiavetti, L. Tognotti, Applied Energy 89 (2012) 203–214.

[23] B. F. Magnussen, in: 19th AIAA Aerospace Science Meeting.

[24] F. C. Christo, B. B. Dally, Combustion and Flame 142 (2005) 117–129.

[25] A. Frassoldati, P. Sharma, A. Cuoci, T. Faravelli, E. Ranzi, Applied Thermal Engineering 30 (2010) 376 – 383.

[26] A. De, E. Oldenhof, P. Sathiah, D. Roekaerts, Flow, Turbulence and Combustion 87 (2011) 537–567.

[27] J. Aminian, C. Galletti, S. Shahhosseini, L. Tognotti, Flow, Turbulence and Combustion 88 (2012) 597–623.

[28] S. R. Shabanian, P. R. Medwell, M. Rahimi, A. Frassoldati, A. Cuoci, Applied Thermal Engineering 52 (2013) 538 – 554.

[29] M. Evans, P. Medwell, Z. Tian, Combustion Science and Technology 187 (2015) 1093–1109.

[30] A. Shiehnejadhesar, R. Mehrabian, R. Scharler, G. M. Goldin, I. Obernberger, Fuel 126 (2014) 177 – 187.

[31] S. Pope, Combustion Theory and Modelling 1 (1997) 41–63.

[32] I. S. Ertesvåg, B. F. Magnussen, Combustion Science and Technology 159 (2001) 213–236.

[33] I. R. Gran, B. F. Magnussen, Combustion Science and Technology 119 (1996) 191–217.

[34] Y. Minamoto, N. Swaminathan, R. S. Cant, T. Leung, Combustion Science and Technology 186 (2014) 1075–1096.

[35] T. Poinsot, D. Veynante, Theoretical and Numerical Combustion, R.T. Edwards, Inc., 2001.

[36] K. Kuo, R. Acharya, Fundamentals of Turbulent and Multi-Phase Combustion, Wiley, 2012.

[37] G. Damköhler, Zs Electrochemie 6 (1940) 601–652.

[38] Y. Minamoto, N. Swaminathan, International Journal of Advances in Engineering Sciences and Applied Mathematics 6 (2014) 65–75.

[39] C. Duwig, L. Fuchs, Combustion Science and Technology 180 (2008) 453–480.

[40] C. Duwig, P. Iudiciani, Fuel 123 (2014) 256 – 273.

[41] B. J. Isaac, A. Parente, C. Galletti, J. N. Thornock, P. J. Smith, L. Tognotti, Energy & Fuels 27 (2013) 2255–2265.

[42] P. J. Roache, Verification and validation in computational science and engineering, Hermosa Publishers, Albuquerque, NM, 1998.

[43] R. Bilger, S. Starner, R. Kee, Combustion and Flame 80 (1990) 135–149.

[44] A. P. Morse, Axisymmetric Turbulent Shear Flows with and without Swirl, Ph.D. thesis, London University, 1977.

[45] C. Bowman, R. Hanson, D. Davidson, J. W.C. Gardiner, V. Lissianski, G. Smith, D. Golden, M. Frenklach, M. Goldenberg, GRI-Mech 2.11, 1995.

[46] G. P. Smith, D. M. Golden, M. Frenklach, B. Eiteener, M. Goldenberg, C. T. Bowman, R. K. Hanson, W. C. Gardiner, V. V. Lissianski, Z. W. Qin, GRI-Mech 3.0, 2000.

[47] C. Westbrook, F. Dryer, Progress in Energy and Combustion Science 10 (1984) 1–57.

[48] W. L. Oberkampf, M. F. Barone, Journal of Computational Physics 217 (2006) 5–38.

[49] F. C. Christo, G. G. Szego, B. B. Dally, in: 5th Asia-Pacific Conference on Combustion, Adelaide, July 2005.

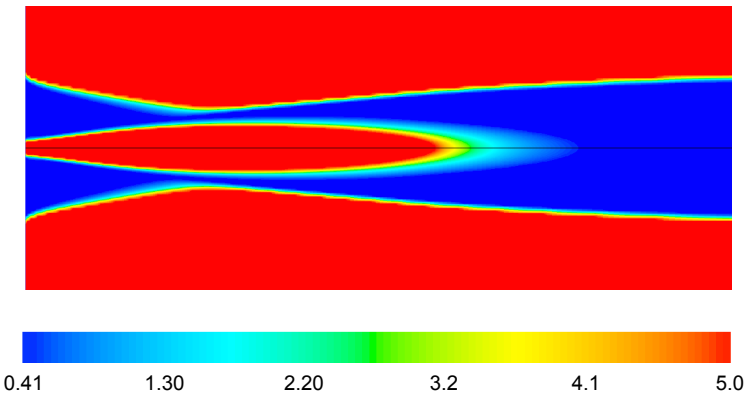

(a) C_τ

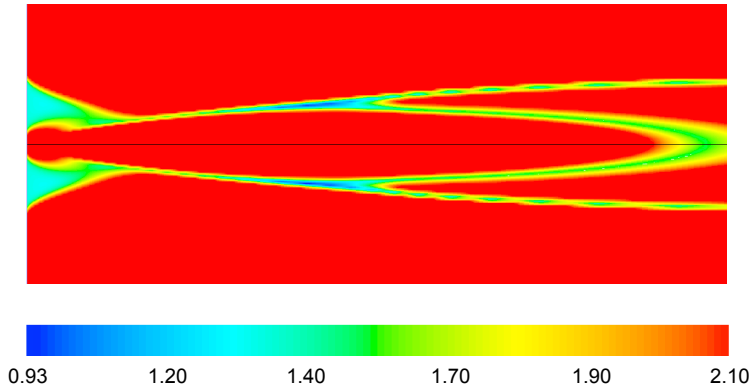

(b) C_γ

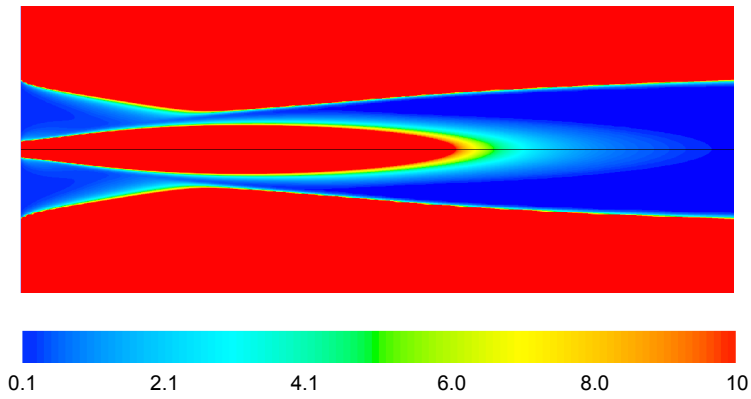

(c) Re^*

Figure 4: Characteristic C_τ (a), C_γ (b) and Re^* (c) distribution for the JHC system. The horizontal axis denotes the axial direction. O_2 level in the co-flow:3%. Fuel-jet Reynolds number:10,000.

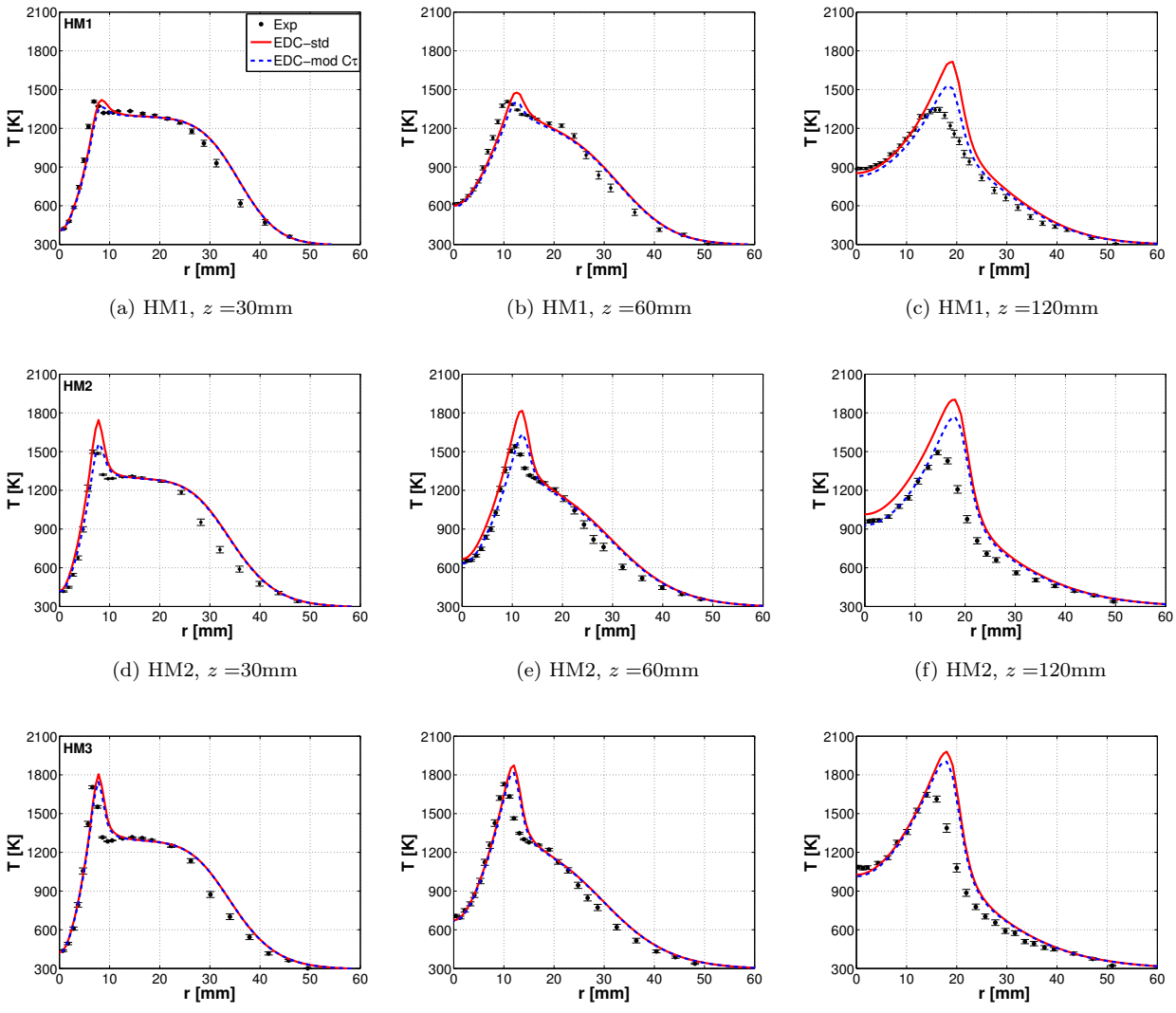

(a) HM1, z =30mm (b) HM1, z =60mm (c) HM1, z =120mm

(d) HM2, z =30mm (e) HM2, z =60mm (f) HM2, z =120mm

(g) HM3, z =30mm (h) HM3, z =60mm (i) HM3, z =120mm

Figure 5: Comparison of measured and computed radial temperature profiles at different axial locations, for flames HM1 (a-c), HM2 (d-f) and HM3 (g-i).

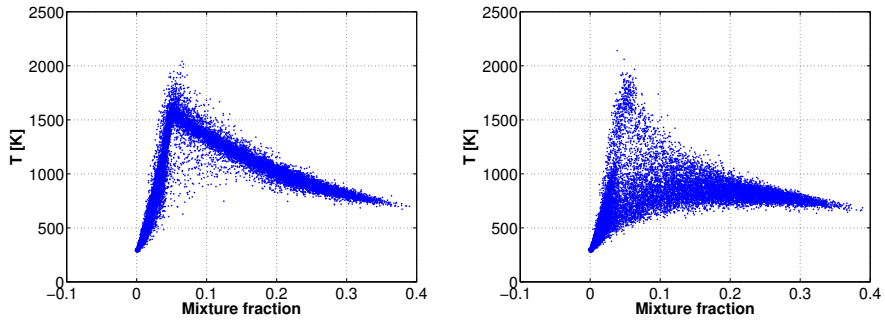

(a) HM1-10k, z = 120mm (b) HM1-20k, z = 120mm

Figure 6: Scatter plots of temperature as a function of the mixture fraction for the Re=10,000 (HM1-10k) (a) and Re=20,000 (HM1-20k) (b) flames.

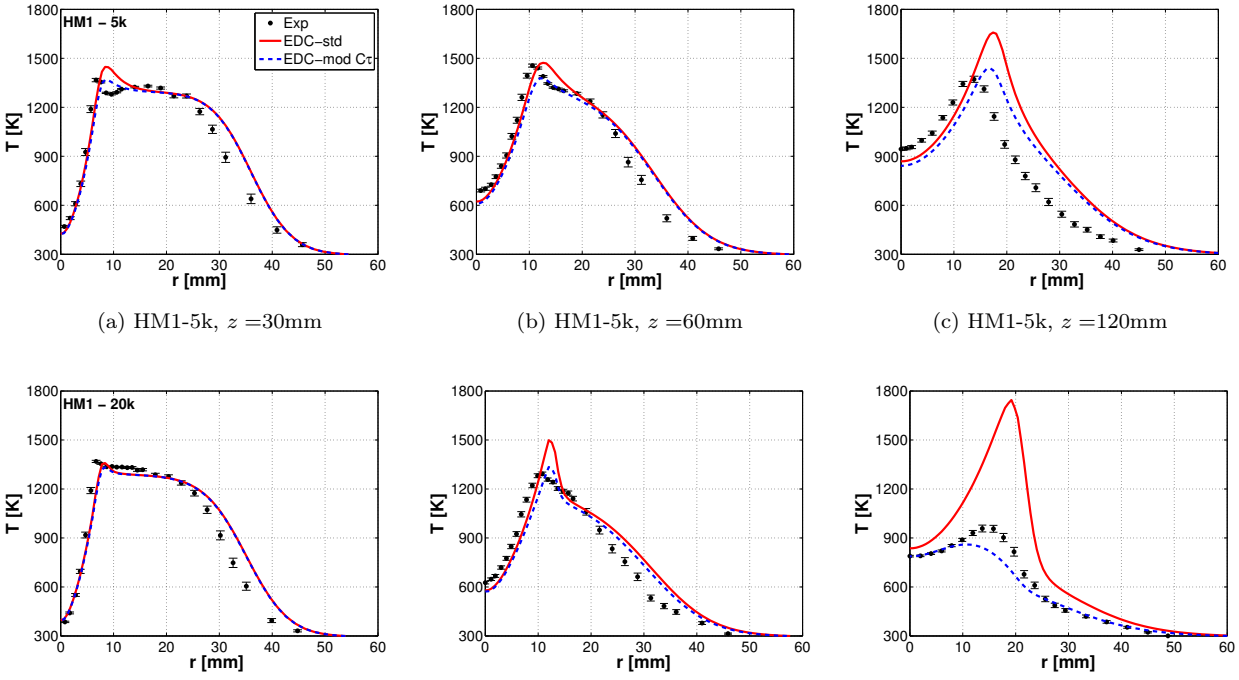

(a) HM1-5k, z =30mm (b) HM1-5k, z =60mm (c) HM1-5k, z =120mm

(d) HM1-20k, z =30mm (e) HM1-20k, z =60mm (f) HM1-20k, z =120mm

Figure 7: Radial temperature profiles at different axial locations along the axis, for flames HM1-5K (a-c) and HM1-20K (d-f).

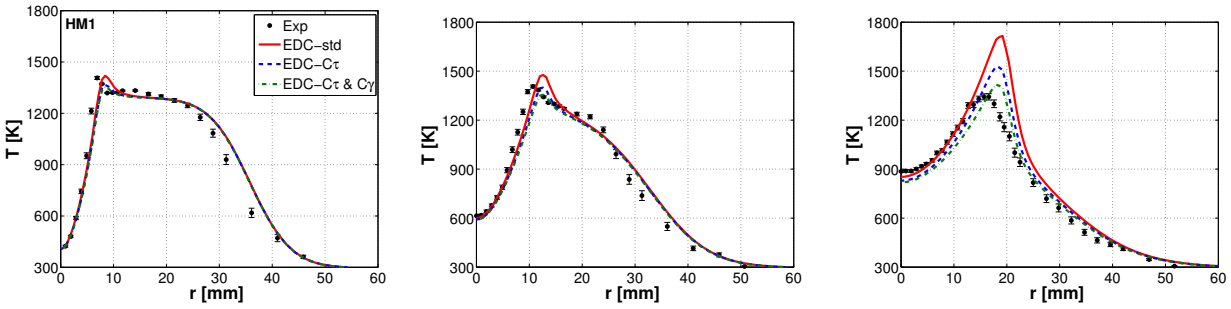

(a) HM1, z =30mm (b) HM1, z =60mm (c) HM3, z =120mm

Figure 8: Radial temperature profiles at different axial locations along the axis for flame HM1, resulting from the simultaneous modification of the EDC coefficients.

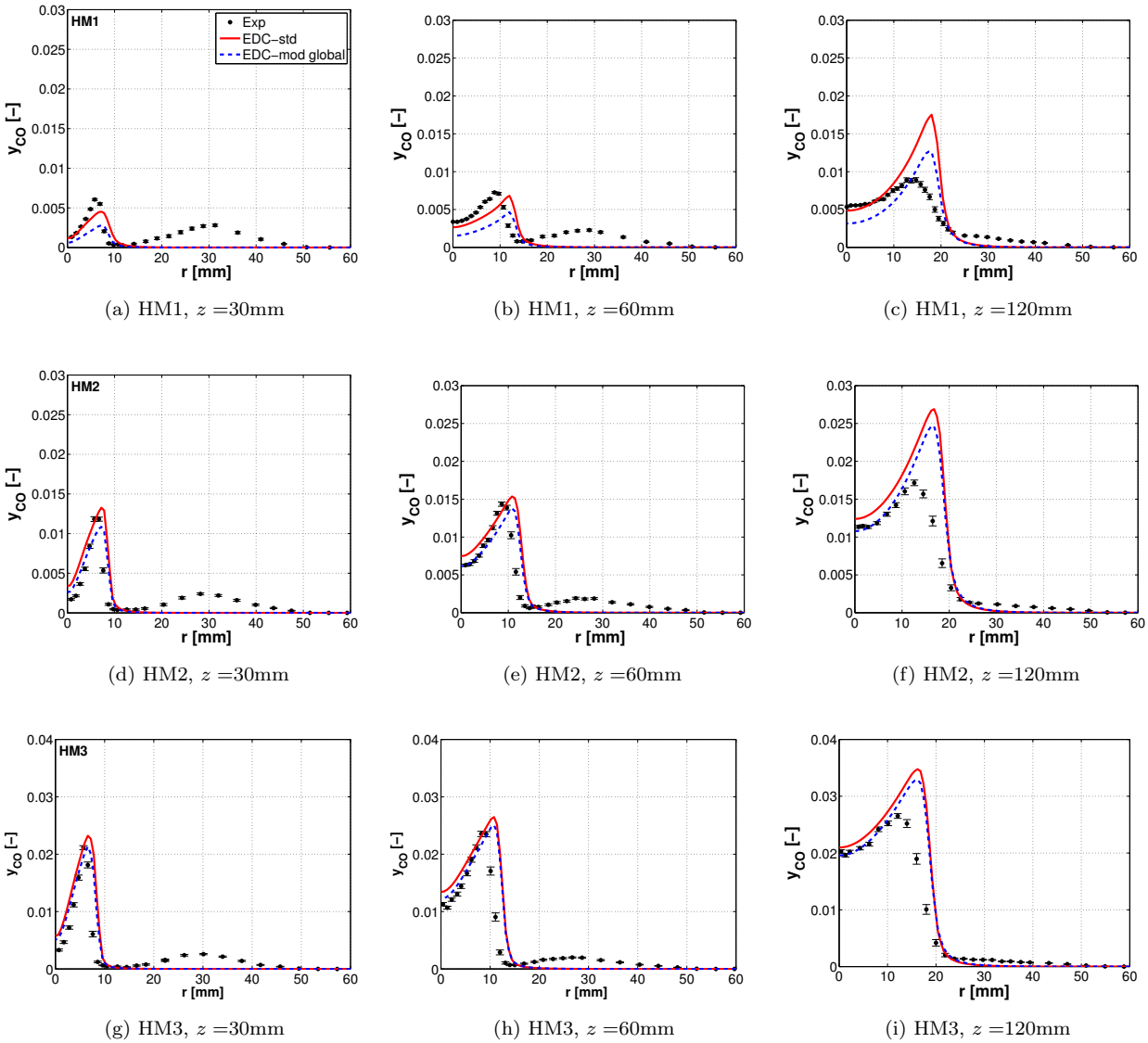

(a) HM1, z =30mm (b) HM1, z =60mm (c) HM1, z =120mm

(d) HM2, z =30mm (e) HM2, z =60mm (f) HM2, z =120mm

(g) HM3, z =30mm (h) HM3, z =60mm (i) HM3, z =120mm

Figure 9: Radial profile of CO mass fraction at different axial locations, for flames HM1 (a-c), HM2 (d-f) and HM3 (g-i).

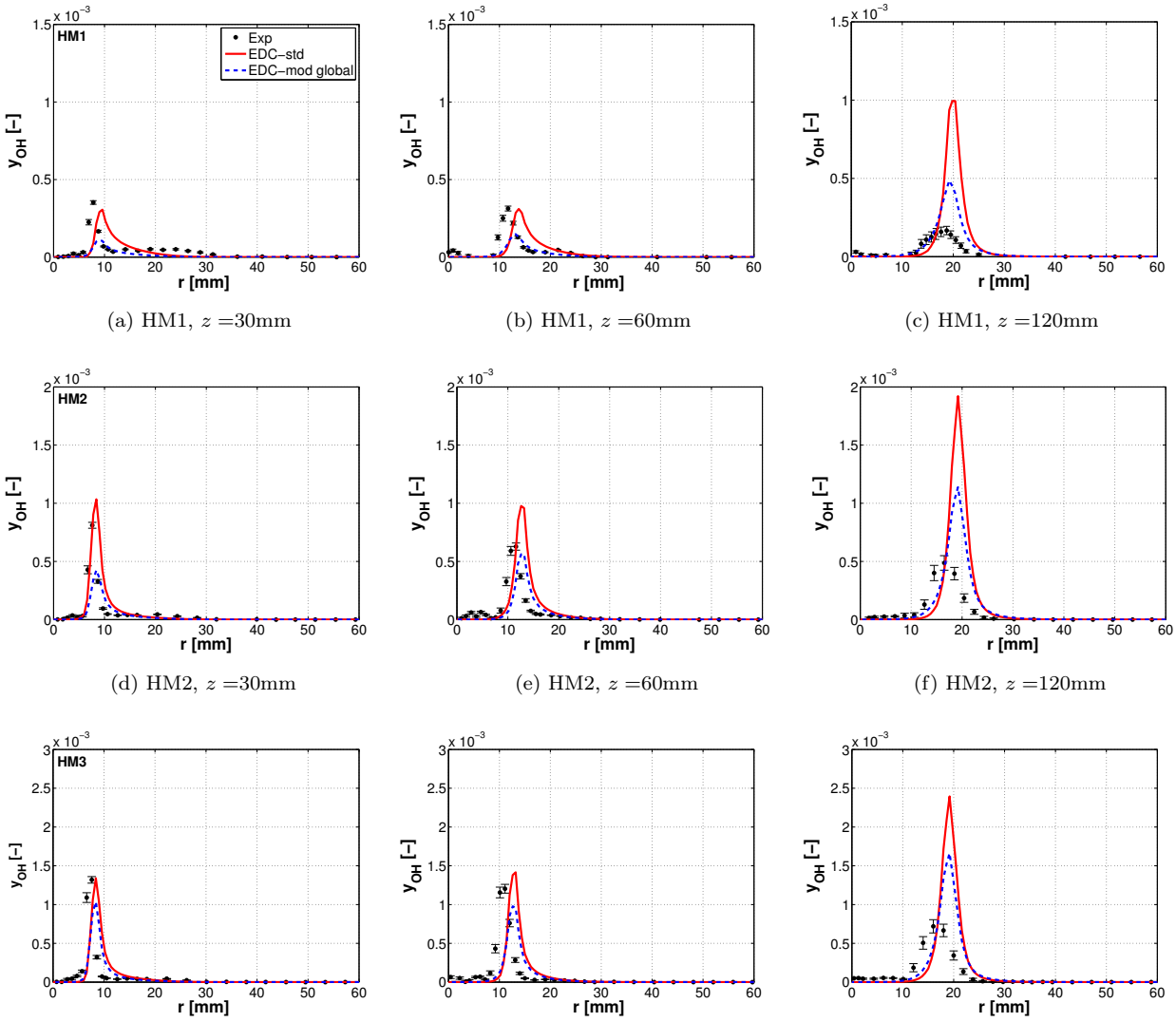

(a) HM1, z =30mm (b) HM1, z =60mm (c) HM1, z =120mm

(d) HM2, z =30mm (e) HM2, z =60mm (f) HM2, z =120mm

(g) HM3, z =30mm (h) HM3, z =60mm (i) HM3, z =120mm

Figure 10: Radial profile of OH mass fraction at different axial locations, for flames HM1 (a-c), HM2 (d-f) and HM3 (g-i).

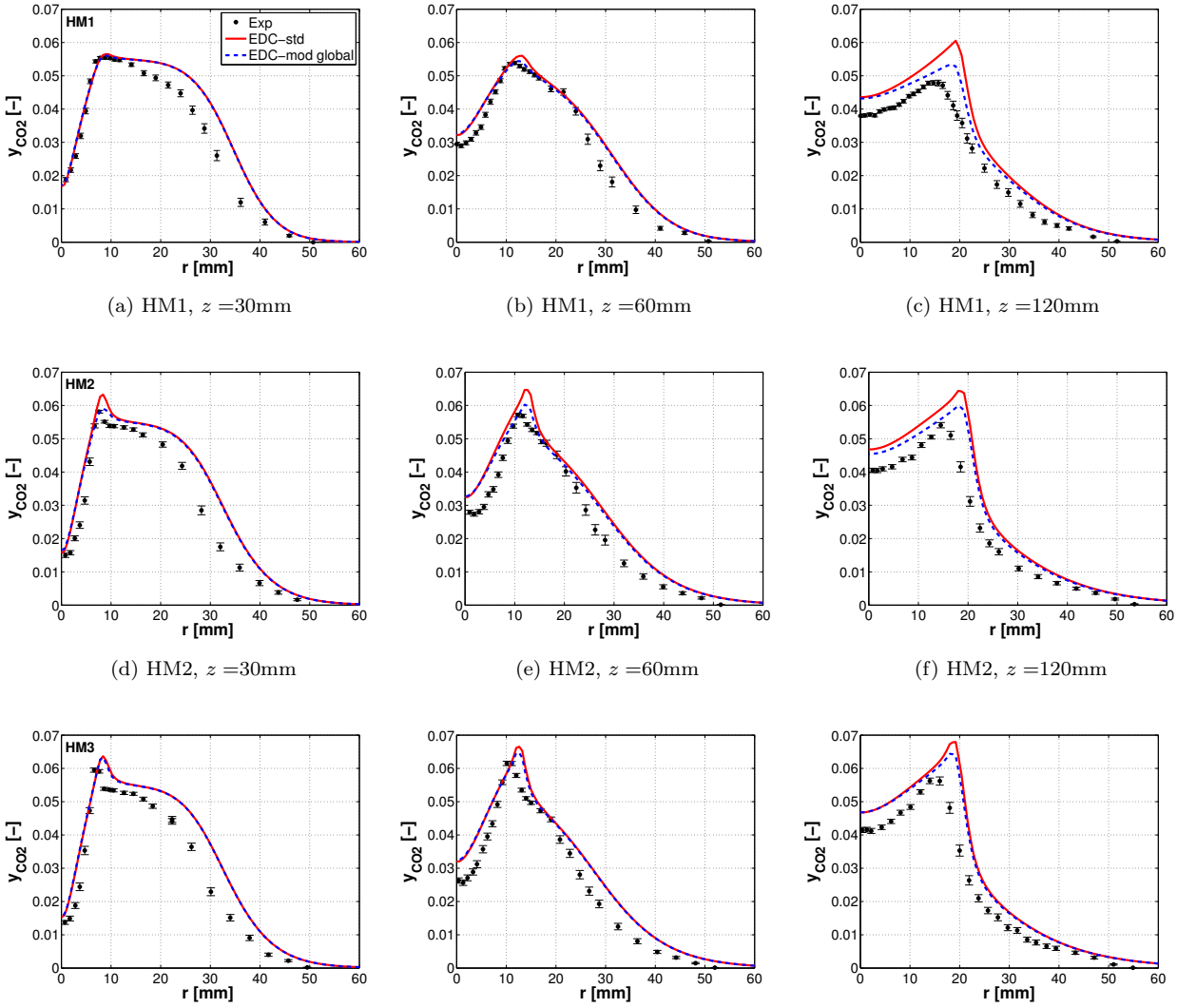

(a) HM1, z =30mm (b) HM1, z =60mm (c) HM1, z =120mm

(d) HM2, z =30mm (e) HM2, z =60mm (f) HM2, z =120mm

(g) HM3, z =30mm (h) HM3, z =60mm (i) HM3, z =120mm

Figure 11: Radial profile of CO2 mass fraction at different axial locations, for flames HM1 (a-c), HM2 (d-f) and HM3 (g-i).

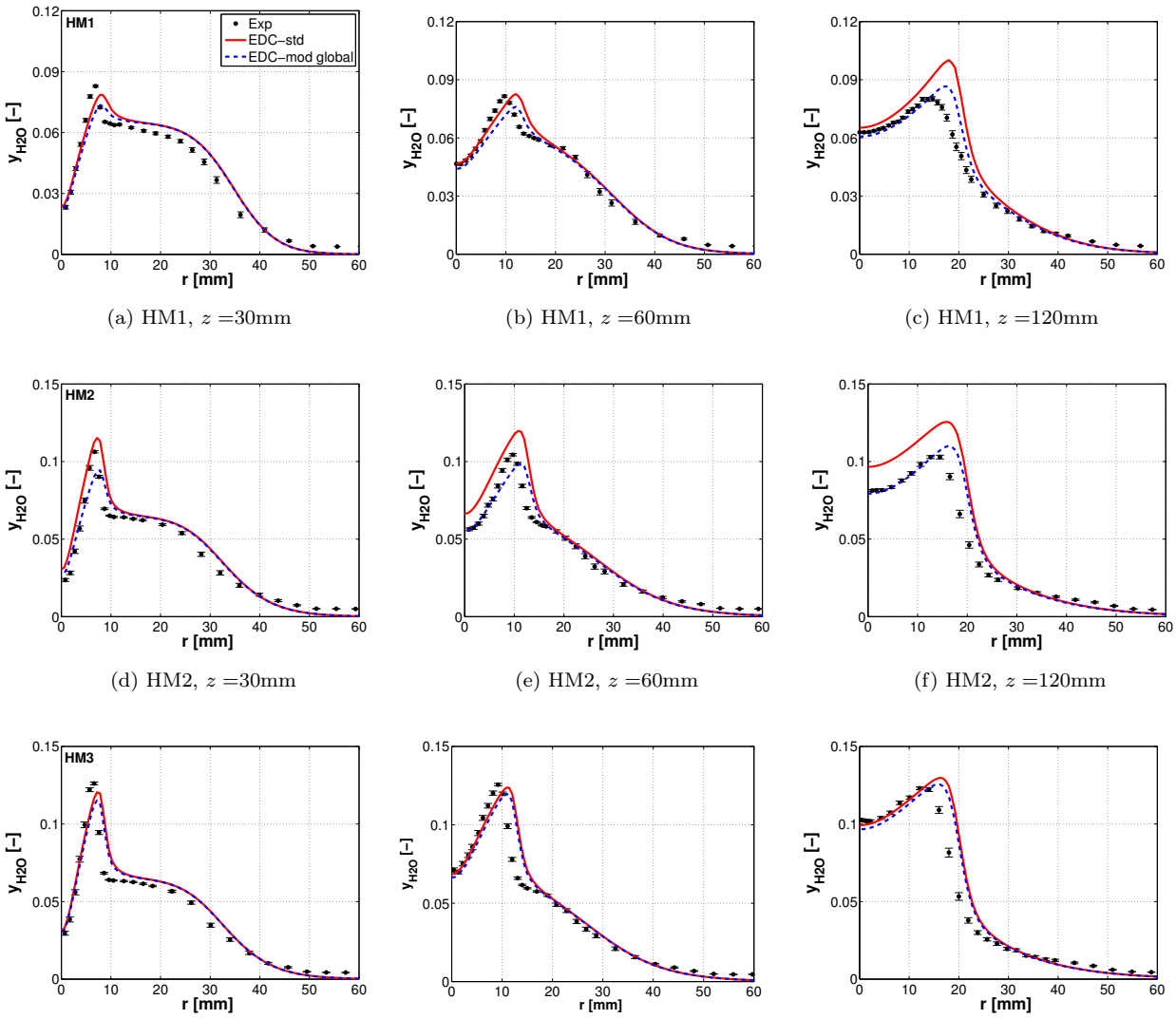

(a) HM1, z =30mm (b) HM1, z =60mm (c) HM1, z =120mm

(d) HM2, z =30mm (e) HM2, z =60mm (f) HM2, z =120mm

(g) HM3, z =30mm (h) HM3, z =60mm (i) HM3, z =120mm

Figure 12: Radial profile of H2O mass fraction at different axial locations, for flames HM1 (a-c), HM2 (d-f) and HM3 (g-i).

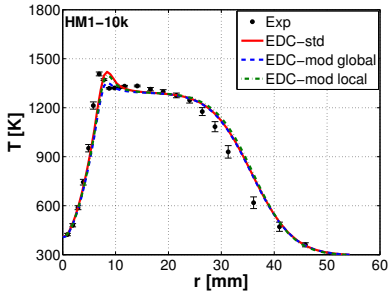

(a) HM1, z =30mm

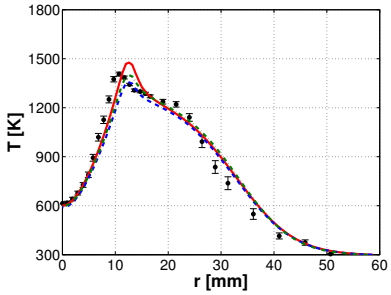

(b) HM1, z =60mm

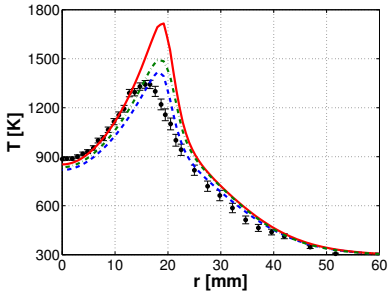

(c) HM1, z =120mm

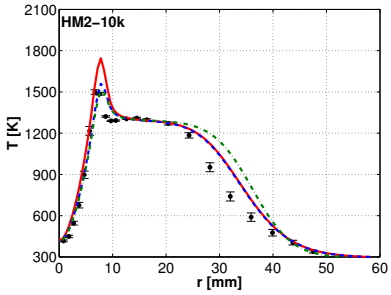

(d) HM2, z =30mm

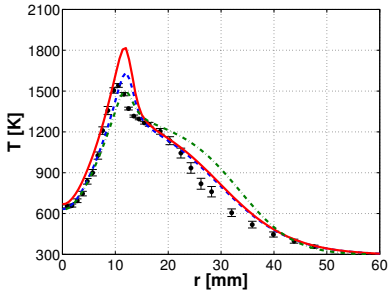

(e) HM2, z =60mm

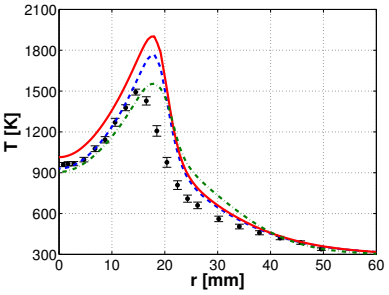

(f) HM2, z =120mm

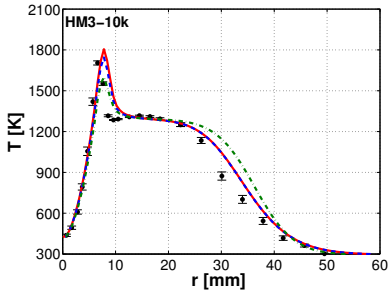

(g) HM3, z =30mm

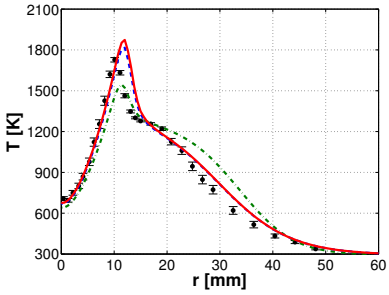

(h) HM3, z =60mm

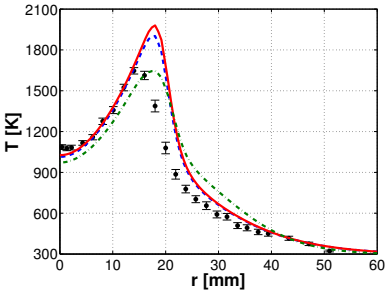

(i) HM3, z =120mm

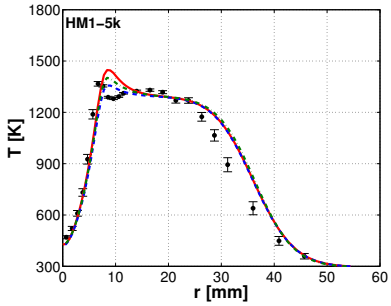

(j) HM1-5k, z =30mm

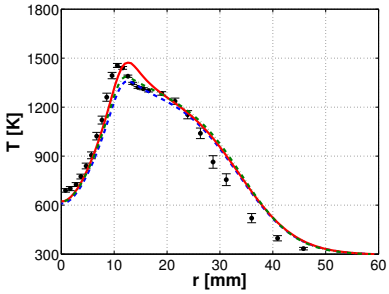

(k) HM1-5k, z =60mm

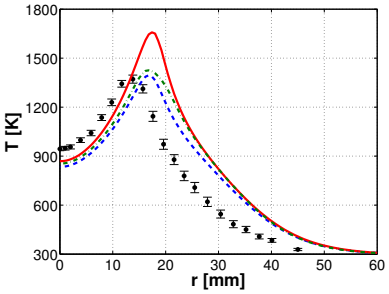

(l) HM1-5k, z =120mm

Figure 13: Radial temperature profiles at different axial locations, for flames HM1 (a-c), HM2 (d-f), HM3 (g-i) and HM1-5k (j-l).

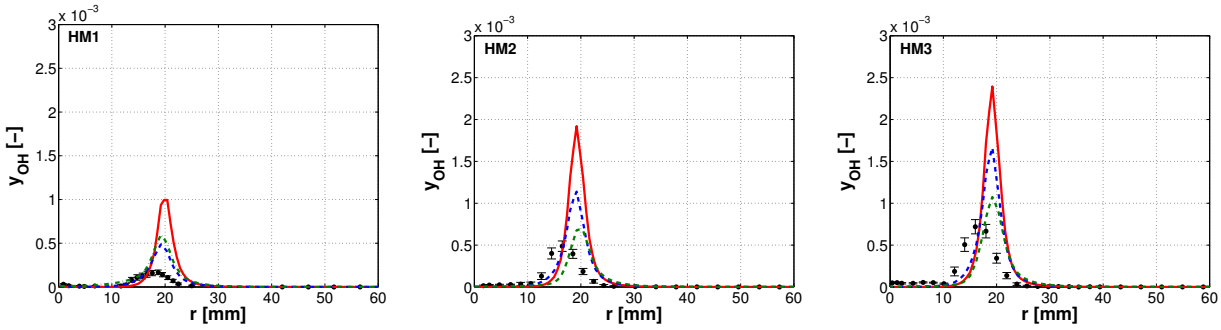

(a) HM1, z =120mm (b) HM2, z =120mm (c) HM3, z =120mm

Figure 14: Radial profiles of OH mass fraction at $z = 120$ mm, for flames HM1 (a), HM2 (b) and HM3 (c).